

Bi-directional electrothermal electromagnetic actuators

Andrew Cao¹, Jongbaeg Kim² and Liwei Lin¹

¹ Berkeley Sensor and Actuator Center, University of California, Berkeley, CA 94720, USA

² School of Mechanical Engineering, Yonsei University, Seoul, Korea

E-mail: kimjb@yonsei.ac.kr

Received 4 January 2007, in final form 8 March 2007

Published 12 April 2007

Online at stacks.iop.org/JMM/17/975

Abstract

A new breed of in-plane bi-directional MEMS actuators based on controlled electrothermal buckling and electromagnetic Lorentz force has been demonstrated under both dc and ac operations. Experimentally, bi-directional actuators made by the standard surface-micromachining process have a lateral actuation range of several microns and can exert forces over 100 μN , while those made by SOI and MetalMUMPs processes have an operation range up to several tens of microns and can exert more than 20 mN of force. Reliability tests show that SOI/MetalMUMPs and surface-micromachined actuators can operate for more than 1 and 100 million cycles, respectively, with no signs of degradation. As such, these micro-actuators could be used for MEMS devices that require a bi-directional movement with a large force output such as bi-directional micro-relays.

(Some figures in this article are in colour only in the electronic version)

1. Introduction

This paper presents a new type of in-plane bi-directional micro-actuator. Many MEMS actuators have been demonstrated in the past utilizing various operation principles such as electrostatic, electrothermal, electromagnetic and shape memory effects. Electrostatic actuators are typically energy efficient but often require high voltages to operate in air [1]. Furthermore, it is difficult to build electrostatic actuators with both large displacement and high force. For example, electrostatic actuators usually have large overlapping areas with compliant suspension structures and operate under resonance to increase output force and deflection [2]. Contact type electrostatic actuators [3–7] can exert much larger force and achieve larger displacements; however, these actuators consist of a dielectric layer and suffer from contact type stiction/failure due to charge leakage and accumulation [8]. Electrothermal actuators such as U-shaped heatuators [9, 10], bent beam actuators [11–13], thermal buckling type [14] as well as single and bi-directional out-of-plane actuators [15] can typically exert larger forces as compared with the electrostatic actuators of similar size. However, they are slow and power hungry as power requirements are generally

in the ranges of several milliwatts, consisting of several volts and several milliamps of currents. Magnetic and electromagnetic actuators come in several types: variable reluctance actuators [16, 17], Lorentz force actuators [18, 19] as well as actuators using permanent magnets [19] and hybrids of these mechanisms. These actuators can exert large force and are capable of large displacements. However, large force often requires large amounts of power and large displacement is usually achieved only by large actuators. The fabrication processes of magnetic actuators are often complicated. Variable reluctance actuators require the use of high permeability materials such as nickel–iron. One or more thick metallic layers are used to make coils, and these layers require high aspect ratio lithography and electroplating processes. Some magnetic actuators use external permanent magnets or electromagnets while others use deposition and patterning of hard magnetic materials in the fabrication process. In addition to the aforementioned actuators, there are actuators using special materials such as piezoelectric materials [20, 21] and shape memory alloys [22]. Incorporating these materials into MEMS fabrication processes can be challenging, as the deposited materials may not exhibit the same desired properties as the bulk materials.

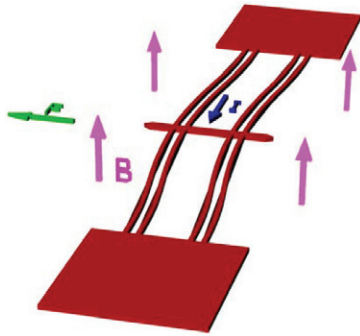


Figure 1. Working principle of the bi-directional, electrothermal, electromagnetic actuator. When an electrical current (I) passes from one pad through the actuation beam to the other pad, the Lorentz force (F) generated by the current interacting with the external magnetic field (B) controls the actuation direction while thermal expansion of beams provides the actuation force.

Actuators can also operate under thermal or electrolysis bubbles [23], osmotic effect [24] or thermal expansion of paraffin wax [25].

The electrothermal–electromagnetic actuators presented in this paper combine both electrothermal and electromagnetic effects to perform bi-directional, in-plane motions. The actuator displacement can be accurately controlled within its entire range of planar movement in contrast to other actuators having bi-directional characteristics that either conduct out-of-plane directions [15, 26] or discrete bi-stable states [27]. Furthermore, these actuators have clamped–clamped bridge designs such that they can be easily built with different microfabrication processes, including surface micromachining, SOI and MetalMUMPs as demonstrated in this work. The bi-directional nature, the ability to accurately move within its displacement range, and the ability to operate under non-resonant conditions, could open up possible opportunities in microsystems.

The original design intent for this bi-directional actuator is to activate micro-relays. The bi-directional capability makes it possible to design relay configurations not possible with mono-directional actuators. The large bi-directional force and displacement make it possible to toggle bi-stable relays. The moving contact of the relay is mounted on a bi-stable mechanism. The actuator would toggle the relay on and off; consuming power only during the switching process. This micro-actuator has been successfully applied in micro-relays, although the bi-stable relays did not work as intended due to some process issues. Another possible application that harnesses the bidirectional nature of the actuator is found in [28], where the capacitance tuning capability of varactor is significantly extended utilizing the extended range of travel. MEMS optical components such as switches and scanners that require a stable and longer travel range can also benefit from this actuator [26]. Yet another application could be mechanical field programmable gate arrays (FPGA).

2. Operating principle

The design concept of the bi-directional, electrothermal, electromagnetic actuator is shown in figure 1. The actuator

is powered by one (or more) clamped–clamped beam fixed between two contact pads that are anchored to the substrate [29]. As electrical current flows through the beam, joule heating causes the beam to expand.

The heat generated can be expressed as

$$P = V^2/R, \quad (1)$$

where V is the applied voltage across the pads and R is the electrical resistance, which in turn can be expressed as

$$R = \rho(T)L/A_c, \quad (2)$$

where $\rho(T)$ is the temperature-dependent resistivity, L is the beam length and A_c is the cross-sectional area. Hence Power can also be expressed as

$$P = V^2 A_c / \rho(T) L. \quad (3)$$

The above equation shows that for a constant voltage input, the heat generated in the actuator depends on how resistivity changes with temperature. If resistivity increases with temperature, as in the case with metal and highly doped silicon, the power dissipated will be self-limiting. Eventually, the rate of heat generation equals the rate of heat dissipation to the environment; hence the actuator will reach a steady state temperature distribution. However, if the resistivity of the actuator decreases with temperature, more and more power will be generated by the actuation beam, until the actuator melts. This is the case with lightly doped silicon as in our SOI actuators. At low temperature, resistivity rises with temperature. Above a critical temperature, the exponentially increasing thermal carriers will cause resistivity to decrease with temperature, leading to actuator meltdown. Within the normal operating range of the actuator, resistivity rises with temperature. Increasing voltage input simply causes the beam to heat up more, leading to a larger lateral displacement. The actuation beams are connected by a cross member in the middle. The dominant heat loss mechanism of this actuator is conduction of heat into the substrate through a thin air gap. The large cross member conducts a lot of heat into the substrate; hence it lowers the temperature at the midpoint of the beam.

As the current flows through the actuation beam, the beam heats up, expands and buckles. The direction of the actuator is not predictable. By placing the actuator in a magnetic field with the field line perpendicular to the buckling direction, the Lorentz force is generated whenever a current flows across the actuation beams as shown in figure 1. The Lorentz force is exerted on a moving charged particle in the presence of a magnetic field:

$$F = qv \times B, \quad (4)$$

where q is the charge on the particle, v is the particle velocity and B is the magnetic flux density. In many engineering applications, the Lorentz force can also be expressed in the form of a current flowing through a conductor interacting with a magnetic field as

$$F = BIL \sin \theta, \quad (5)$$

where I is the current and θ is the angle between the current and the magnetic field. The Lorentz force controls the buckling direction of the beam. When the current direction is switched, the Lorentz force is reversed and the beam buckles in the opposite direction. Experimentally, it is found that the Lorentz force generated is large enough to consistently control the buckling direction. However, its contribution to the overall displacement of the actuator is relatively small.

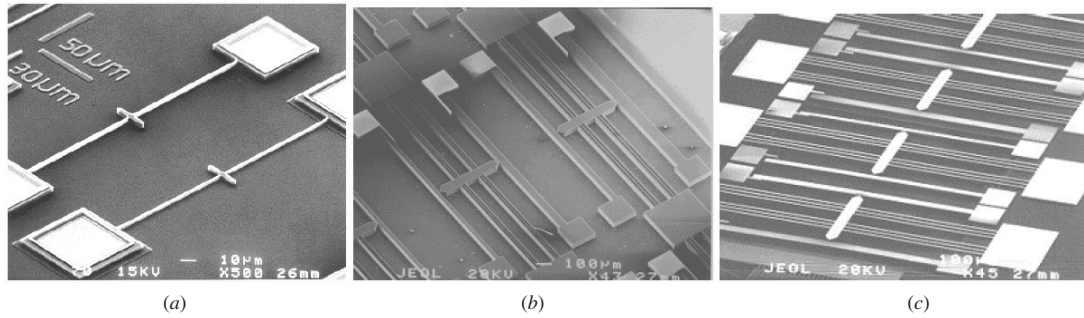


Figure 2. SEM micrographs of (a) two single-beam bi-directional actuators made using the PolyMUMPs process. The top actuator is $3.5 \mu\text{m}$ in thickness; the bottom actuator is $2 \mu\text{m}$ in thickness. (b) Actuators made using a $50 \mu\text{m}$ thick SOI process with a $1 \mu\text{m}$ thick buried oxide layer. These actuators have an actuation beam length of $2000 \mu\text{m}$ and widths ranging from 5 to $15 \mu\text{m}$. (c) MetalMUMPs bi-directional actuators.

3. Actuator design and fabrication

These bi-directional, electrothermal, electromagnetic actuators can be fabricated with a process with one or more suspended, electrically conducting structural layers. This paper presents results from polysilicon surface micromachining, $50 \mu\text{m}$ thick SOI and $20 \mu\text{m}$ thick electroplated nickel processes.

3.1. PolyMUMPs actuators

The polysilicon surface-micromachined actuators are made using the PolyMUMPs process [30]. The actuation beams could be made using either the $2.0 \mu\text{m}$ Poly1 layer, the $1.5 \mu\text{m}$ Poly 2 layer or a combination of both the Poly 1 and Poly 2 layer with a combined thickness of $3.5 \mu\text{m}$. Figure 2(a) shows the SEM photo of two fabricated PolyMUMPs actuators and they follow the design rules of the PolyMUMPs process. It is highly desirable for the actuation beams to have a larger height than its width, since the desired range of motion is in the planar direction. However, the minimum line/space in the PolyMUMPs process is $2 \mu\text{m}/2 \mu\text{m}$ such that actuators built using this process have $2 \mu\text{m}$ wide beams and multiple beam actuators have at least $4 \mu\text{m}$ of spacing between adjacent beams. The typical beam length is $200 \mu\text{m}$.

3.2. SOI actuators

The SOI actuators are fabricated using a $50 \mu\text{m}$ thick p-type structural layer with a $1 \mu\text{m}$ thick insulating oxide as shown in figure 2(b). First, a layer of thermal oxide was grown on the SOI to serve as a hard mask. The actuators were patterned and etched using a single mask by a deep reactive ion-etching machine. The minimum feature size achieved for this process was roughly $5 \mu\text{m}$ for both line and space, with an etch aspect ratio of roughly 50:1. Conservatively, a minimum line/space of $10 \mu\text{m}$ was assumed. The beams were $2000 \mu\text{m}$ long, and had a beam width from $5 \mu\text{m}$ to $15 \mu\text{m}$. The SOI actuators were released using a 49% HF etch followed by a 15 min dip in DI (deionized water), 15 min dip in IPA, then were dried using the super critical CO_2 drying process.

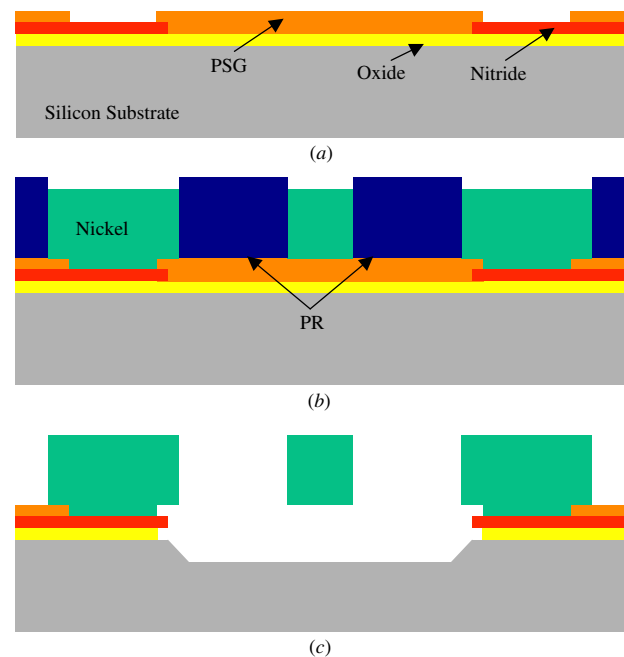


Figure 3. Key steps in MetalMUMPs to make trenched actuators. (a) Deposit $2 \mu\text{m}$ isolation oxide, $0.7 \mu\text{m}$ silicon nitride; pattern nitride to create trench area; deposit $1 \mu\text{m}$ PSG, pattern PSG. (b) Blank deposit of seed layer; deposit and pattern PR mold; electroplate $20 \mu\text{m}$ nickel and $0.5 \mu\text{m}$ gold (not shown) structural layer. Nickel on top of nitride would be anchored to the substrate, while nickel plated on top of PSG will be suspended after release. (c) Remove PR; release structures using HF. Etch $25 \mu\text{m}$ trench into the silicon substrate using KOH.

3.3. MetalMUMPs actuators

Two variations of electroplated nickel actuators have been made using the MetalMUMPs process. The actuators could be built directly over a silicon nitride isolation layer with a $1 \mu\text{m}$ air gap, or over a $25 \mu\text{m}$ deep trench, which is etched into the substrate as shown in figure 2(c). The MetalMUMPs process uses a six-mask process with eight thin film layers but not all of the masks and layers are needed to fabricate the bi-directional actuators. The key fabrication process steps to make trenched actuators are shown in figure 3. Thermal isolation trenches are formed by opening windows in the silicon nitride layer, and KOH is used to etch $25 \mu\text{m}$ into the substrate. These trenches

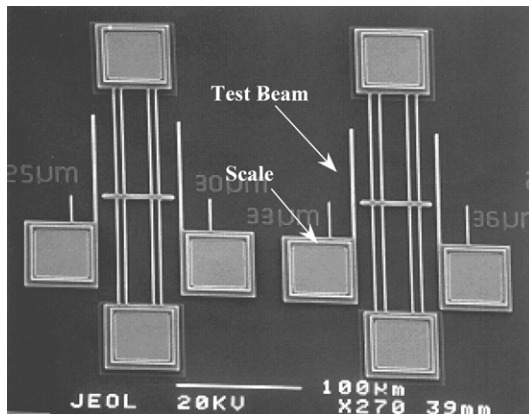


Figure 4. SEM of PolyMUMPs bi-directional actuators and their force testing structure. These 200 μm long, 2 μm wide and 3.5 μm thick actuators have four actuation beams. A bi-directional displacement of 3.5 μm could be achieved under 4 V and 10 mA and the maximum measured force output is 200 μN .

can help prevent heat loss to the substrate and reduce power consumption for these actuators. The MetalMUMPs actuators have to be made relatively big since the minimum line width and space for the nickel structural layer is 8 μm . Practically, we have found that 10 μm line and 30 μm space are necessary to have successfully operable actuators from the MetalMUMPs process. The typical length of the MetalMUMPs actuators is 2000 μm .

3.4. Force testing setup

The force outputs of the actuators were experimentally tested by having the actuators push against cantilever beams built adjacent to the actuator as shown in figure 4. The force exerted by the actuator could be calculated from the measured displacement of the cantilever beam tip using beam theory:

$$F = \frac{-6y_A EI}{(2L^3 - 3L^2a + a^3)}, \quad (6)$$

where F is the force exerted, y_A is the deflection at the free end and a is the distance between the free end and where the force is applied. A scale indicates the distance between the cantilever beams' anchor and the point where the force is applied; this scale can also be used to calibrate microscope measurements. The width of the cantilever beam and location where the force is applied can be designed for successive tests for more accurate measurements.

4. Results and discussions

These actuators are tested by placing them on top of a 1 inch diameter, 0.25 inch thick, permanent magnet with a 0.3 T flux density. There are three operating regions. First, when a small alternating voltage is applied, no noticeable movement could be seen for silicon actuators because the beam did not reach the buckling state. MetalMUMPS actuators can interact with the magnetic field much better than silicon actuators to have a small movement due to the Lorentz force. By using equation (5), the estimated Lorentz force for a MetalMUMPs actuator under a current of 1 A is 600 μN which is significant for microscale operations. The deflection caused by the

Lorentz force is 3.5 μm , which is about 1/10 of the maximum bi-directional displacement amplitude in operation. Second, once the voltage is raised beyond a critical voltage where the beams start to buckle, the actuators suddenly move with noticeable amplitude. As the applied voltage increases, the amplitude of movement increases and this is the desired region of operation. The operation details in this region due to buckling of beams have been previously reported with mathematical derivations, computer simulation and experimental verifications on a polysilicon structure [29]. Third, under high voltage, actuators start to deform permanently due to a combination of heat and stress. In this region, actuators deflect in one random direction and function as a mono-directional actuator when the Lorentz force is not high enough to overcome some permanent shape change caused by heat and stress. As the applied power is increased even higher, the actuators start to visibly deform, soften and gradually melt.

Actuators with a single actuation beam tend to fail by out-of-plane twisting. Therefore, actuators with at least two widely spaced beams connected in the middle with a cross member have been adopted to overcome possible twisting moments. Without the cross member, the hottest region in a clamped-clamped beam would be at the center of the beam. With the cross member, the hottest region typically moves to about midway between the pads and the cross member.

4.1. Characterization of PolyMUMPS actuators

Two generations of surface-micromachined actuators have been fabricated using the PolyMUMPs foundry service. These actuators have one to four actuation beams with a thickness of 2 μm or 3.5 μm , width of 2 μm and length of 200 μm . The nominal resistivity of polysilicon layers from the PolyMUMPs run is 20 Ω/\square . Figure 5 shows the I - V curves and the power versus displacement curves of several tested PolyMUMPs actuators. The typical operating voltages of the surface-micromachined bi-directional actuators are between 0 and 10 V, and the corresponding current ranges from 2 to 15 mA, depending on the number of actuation beams and actuator thickness. The performance of the bi-directional actuators is comparable to other thermal actuators. For example, a U-shaped heater with 240 μm long cold arm can achieve a 16 μm displacement with 3 V and 3.5 mA [9]. An 800 μm long polysilicon bent beam actuator can displace about 5 μm at 12 V and 14 mA [11].

It is noted that 3.5 μm thick actuators actually carry less current than their 2 μm thick counterparts under the same applied voltage. This seems to be against the common sense because thicker actuators should have lower resistance to carry a higher current. It is found that an insulating oxide was left between the Poly1 and Poly2 layers in the PolyMUMPs process. Therefore, electrical current only travels through the top Poly2 layer, which is thinner than the Poly1 layer.

The maximum bi-directional displacement of these actuators is about 4 μm . Actuators deform permanently under higher input power and become mono-directional actuators afterward. This transformation from bi-directional actuators to mono-directional actuators can be seen as a failure mode for bi-directional actuators. However, it can also be seen as the

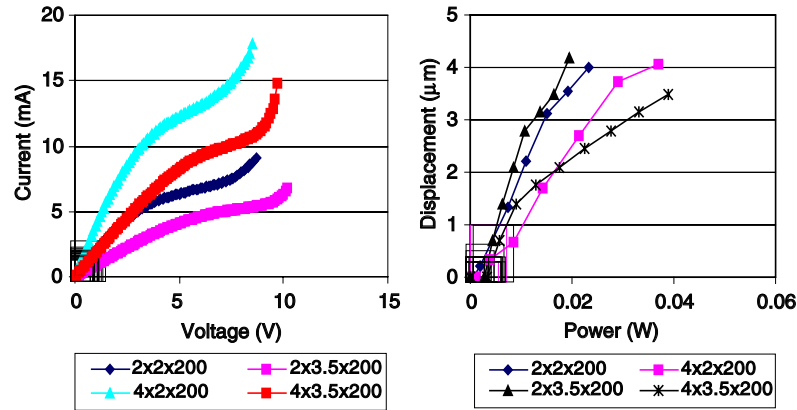


Figure 5. Left: I - V curves of PolyMUMPs actuators. All beams are $2\ \mu\text{m}$ wide, $200\ \mu\text{m}$ -long and 2 or $3.5\ \mu\text{m}$ thick. The $3.5\ \mu\text{m}$ thick actuators carry less current for the same applied voltage than the $2\ \mu\text{m}$ actuators due to the insulating thin oxide layer between the Poly1 and Poly2 layers. Right: power versus displacement curves of the PolyMUMPs bi-directional actuators.

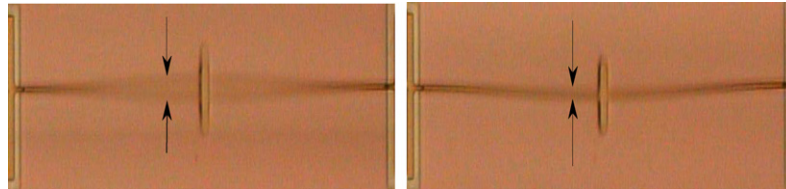


Figure 6. Left: actuator moving through the full range of bi-directional motion and (right) limited to one direction only.

mechanism to make programmable actuators with potential to be used as a FPGA. Previous researchers have tried to use MEMS switches as mechanical logic gates [31]. In this case, the bi-directional actuators could be permanently programmed into desired mono-directional actuators in the presence of a magnetic field.

Heat dissipation determines how fast the bi-directional actuators can move. These actuators were actuated using a sine-shaped alternating current (ac) passing through the actuation beams. In order for the actuator to move in alternating directions, the actuators must cool down to its neutral position, before it is actuated again in the opposite direction. If the alternating frequency is faster than the actuator's thermal response time, the actuators are confined to move in one direction from the neutral position as shown in figure 6. The maximum operating frequency with a bi-directional movement of the surface-micromachined actuator versus input voltage is shown in figure 7. As expected, the maximum operating frequency decreases with increasing voltage because under a high power input, it takes more time for the actuators to cool down. In general, the ac operation range of these bi-directional actuators is less than 5 kHz. At a very high frequency, the alternating current looks more and more like a dc current; hence the actuator stays in one position.

4.2. Characterization of SOI actuators

The SOI actuators consume a lot more power than the PolyMUMPs actuators due to their sizes. The nominal resistivity of the silicon device layer for the SOI wafer is $1.25\ \Omega/\square$. Figure 8 shows the I - V curves of the SOI actuators. The typical operating range is 0–30 V and 20–140 mA, depending on the number and width of the

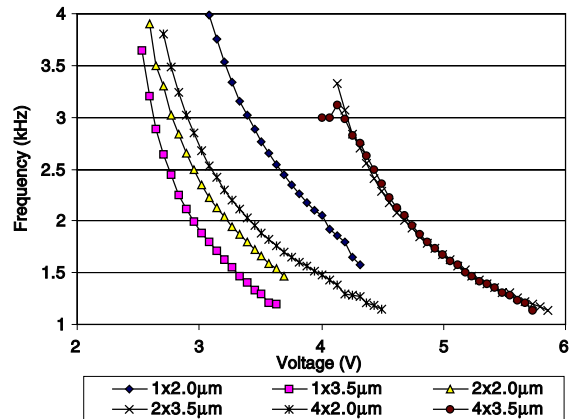


Figure 7. Maximum bi-directional operating frequency versus input voltage of PolyMUMPs surface-micromachined actuators.

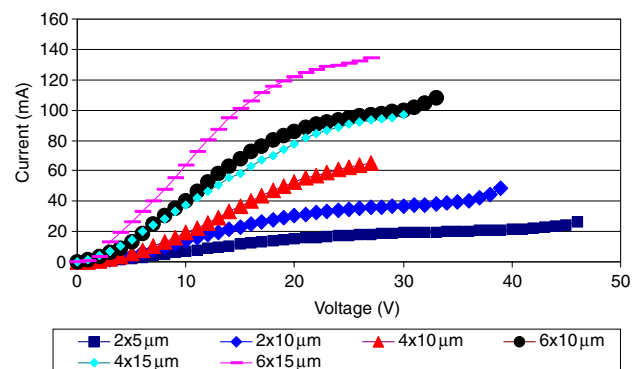


Figure 8. I - V characteristics of SOI bi-directional actuators.

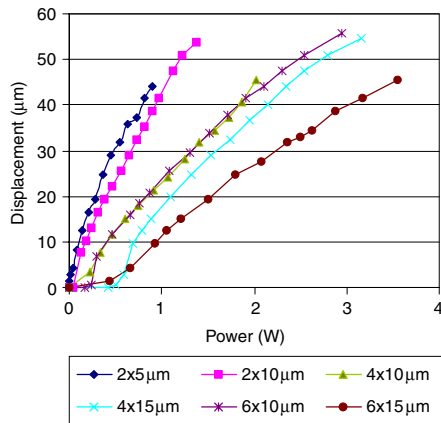


Figure 9. Power versus displacement curves of bi-directional actuators made from 50 μm thick SOI. Actuators have two to six actuation beams ranging from 5 to 15 μm in beam width. The maximum bi-directional displacement is around 40 μm. Note that some actuators with 15 μm wide beams show no displacement at low power and abruptly move as the beams start to buckle.

actuation beams. The maximum operating point is where the actuators attain their maximum bi-directional displacement. The SOI actuators typically fail catastrophically shortly after the actuators passing the maximum operating points. It is believed that the intrinsic carriers, which grow exponentially with temperature, quickly decreased the resistivity of silicon. This results in positive feedback as more current can pass through the actuation beams under the same applied voltage, leading to catastrophic failure. The same phenomenon is not seen in the PolyMUMPs actuators because the poly layers have a much higher doping level; hence the effect of the thermally generated intrinsic carriers is less obvious. However, increments of current toward the tail ends of the *I-V* curves for both types of silicon actuators can be observed in figures 5 and 8.

The power versus displacement curves of the SOI actuators are shown in figure 9. SOI actuators can move bi-directionally around 40 μm. Beyond that, actuators show signs of permanent deformation as the neutral position of the actuator shifts by a couple of microns, and the actuator is confined to a mono-directional movement in the direction of the shift. As a mono-directional actuator, these actuators can

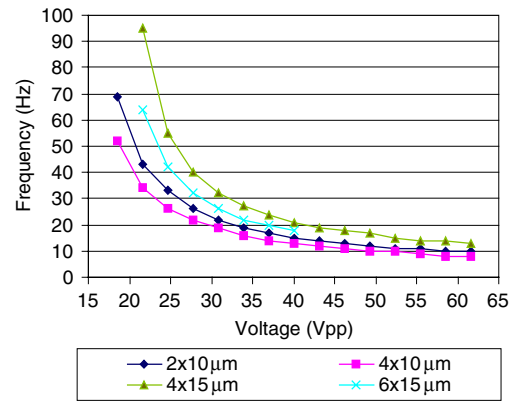


Figure 10. Maximum bi-directional operating frequency versus actuation voltage of 50 μm thick SOI actuators.

displace over 50 μm from the neutral position. The maximum operating frequency versus voltage of the SOI actuators is shown in figure 10. It is observed that SOI actuators are much larger, and they take longer to cool down; hence the operating frequencies are much lower than the surface-micromachined actuators in the tens of hertz.

4.3. Characterization of MetalMUMPs actuators

The MetalMUMPs actuators are designed after one of the most successful SOI actuators with two sets of three-actuation beams of length 2000 μm and width 10 μm as shown in figure 2(c). The MetalMUMPs actuators are more energy efficient than the SOI and polysilicon actuators because the coefficient of thermal expansion (CTE) of nickel, 13×10^{-6} , is much larger than that of silicon at 2.3×10^{-6} . As a result, the same displacement can be achieved under a lower temperature variation. On the other hand, the maximum operating temperature of nickel is about 350 °C, whereas polysilicon can operate up to 600 °C before plastic deformation may occur [11].

The trenched actuators provide even better energy conservation, as the trench insulates the actuator against heat conduction down to the substrate. *I-V* curves and displacements versus power curves of the MetalMUMPs actuators are shown in figure 11. These actuators can achieve a lateral deflection over 80 μm with less than 3 V for the

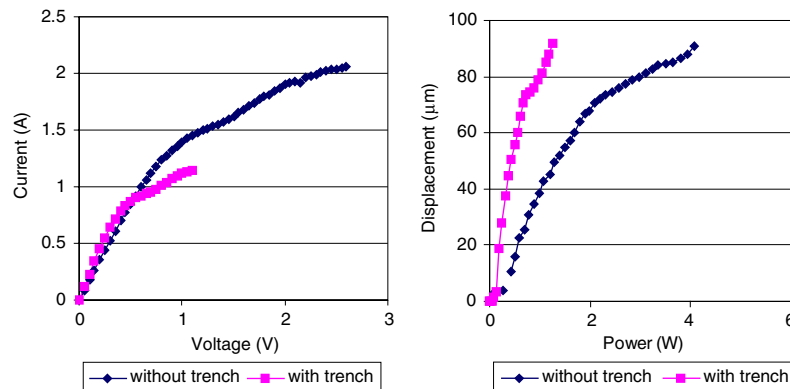
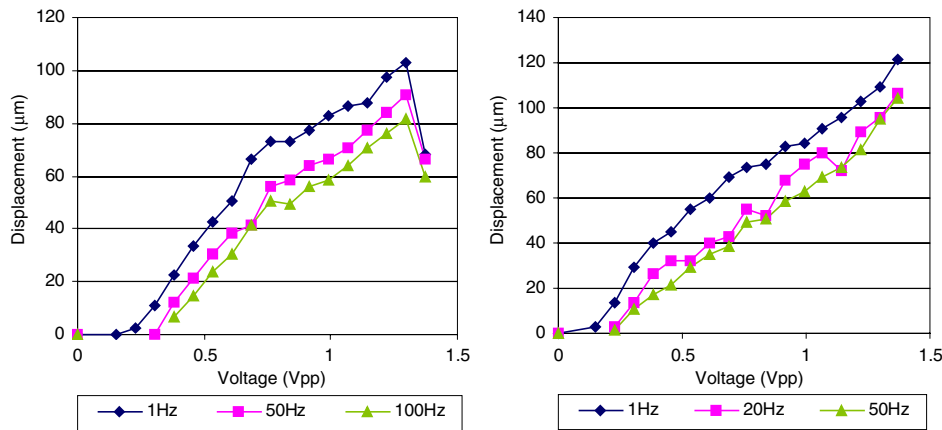


Figure 11. Left: *I-V* curve of trenched and non-trenched MetalMUMPs bi-directional actuator. Right: power versus displacement curve of MetalMUMPs bi-directional actuators.

Table 1. Summary of force measurements of PolyMUMPs, MetalMUMPs and SOI bi-directional actuators.

Process type	Length \times width \times thickness (μm)	No of beams	Highest force output (μN)
PolyMUMPs	$200 \times 2 \times 2$	1	43
PolyMUMPs	$200 \times 2 \times 2$	2	73
PolyMUMPs	$200 \times 2 \times 3.5$	1	124
PolyMUMPs	$200 \times 2 \times 3.5$	2	144
MetalMUMPs	$2000 \times 10 \times 20$ (no trench)	6	3 730
MetalMUMPs	$2000 \times 10 \times 20$ (trenched)	6	2 447
SOI	$2000 \times 10 \times 50$	4	1 830
SOI	$2000 \times 10 \times 50$	6	5 700
SOI	$2000 \times 15 \times 50$	4	20 600

**Figure 12.** Left: non-trenched MetalMUMPs actuator voltage versus displacement curves. As actuation frequency increases, the amplitude of displacement decreases. Right: trenched MetalMUMPs actuator voltage versus displacement curves. Note that the frequencies used for the trenched actuators are lower than the non-trenched actuators.

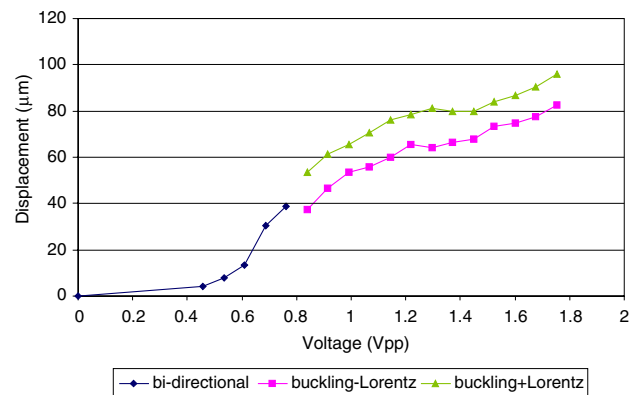
non-trenched actuators and less than 1.5 V for the trenched actuators. The maximum bi-directional displacement of $40 \mu\text{m}$ can be achieved with less than 1 V and 0.5 V for the non-trenched and trenched actuators, respectively. The current requirement, on the other hand, is relatively high in the range of 0.5–1.5 A.

The displacement achieved for a given voltage is frequency dependent. Figure 12 shows the voltage versus displacement curves for trenched and non-trenched actuators at different actuation frequencies. As frequency increases, the amplitude decreases because the energy dissipation process cannot catch up. At a very low frequency, the actuator can reach a quasi steady state. The tested frequencies used for the trenched actuator are lower than the non-trenched actuator because the thermal response rate is slower.

The Lorentz forces generated in the MetalMUMPs actuators are much larger than the SOI or PolyMUMPs actuators and figure 13 illustrates this phenomenon. At low voltages, actuators move in both directions with same amplitude. After permanent deformation occurs at about $40 \mu\text{m}$ of displacement, the actuator can only move in one direction. However, the amplitude of movement alternates between high and low curves with a difference of several microns due to the Lorentz force. This is because in alternating cycles, the Lorentz force either adds or subtracts from the buckling displacement.

4.4. Actuator result summary

The force outputs of the bi-directional actuators were experimentally measured by having the actuator push against

**Figure 13.** Voltage versus displacement measurements for MetalMUMPs actuators before and after permanent deformation at around $40 \mu\text{m}$ of displacement. The amplitude of movement alternates between high and low states with a difference of several microns due to the Lorentz force in two opposite directions.

cantilever beams with known dimensions. Each testing setup has two cantilever beams with different stiffness, which could be controlled by varying beam width and the point at which the beam is pushed. PolyMUMPs actuators can exert a force over $100 \mu\text{N}$, the MetalMUMPs actuators could exert several millinewtons and the strongest SOI actuator can exert over 20 mN. Table 1 summarizes the force output of the PolyMUMPs, MetalMUMPs and SOI actuators.

All three types of actuators show very good mechanical characteristics. In an effort to characterize fatigue strength,

these actuators have been tested using a sine-shaped alternating current close to the point of maximum bi-directional displacements. The PolyMUMPS actuators have been tested for over 100 million cycles at an operating frequency of 1 kHz without failure. The SOI and MetalMUMPS actuators have been tested over 1 million cycles at 10 Hz. In all cases, the tests were stopped due to time constraints, and not because of sample failure.

5. Conclusion

Bi-directional electrothermal electromagnetic actuators have been designed, fabricated and characterized using surface micromachining, SOI and MetalMUMPS processes. These actuators require relatively low voltages and high currents to operate and can exert large forces of more than 20 mN by large actuators made from SOI and MetalMUMPS processes. Actuators made from all three processes are durable and can be used in MEMS applications that require high displacement, high force and bi-directional actuation. The original design intent for these actuators was for MEMS relays. The large bi-directional force would allow for the design of relay configurations not possible with mono-directional actuators. We have successfully made micro-relays with low contact resistance in the MetalMUMPS process using these bi-directional actuators [32]. Other possible applications with these actuators include tunable capacitors or optical components, where movement is needed on both sides of the neutral position.

References

- [1] Tang W C, Nguyen T C H and Howe R T 1989 Laterally driven polysilicon resonant microstructures *Sensors Actuators* **20** 25–32
- [2] Kim J, Christensen Dane and Lin L 2005 Monolithic 2-D scanning mirror using self-aligned angular vertical comb drives *IEEE Photonics Technol. Lett.* **17** 2307–9
- [3] Minami K, Kawamura S and Esashi M 1993 Fabrication of distributed electrostatic micro actuator (DEMA) *J. Microelectromech. Syst.* **2** 121–7
- [4] Shikida M and Sate K 1997 Fabrication of an s-shaped actuator *J. Microelectromech. Syst.* **6** 18–24
- [5] Akiyama T, Collard D and Fujita H 1997 Scratch drive actuator with mechanical links for self-assembly of three-dimensional MEMS *J. Microelectromech. Syst.* **6** 10–7
- [6] Gilbert J R and Senturia S D 1996 Two-phase actuators: stable zipping devices without fabrication of curved structures *Proc. 7th IEEE Solid-State Sensor and Actuator Workshop* pp 98–100
- [7] Legtenberg R, Gilbert J and Senturia S D 1997 Electrostatic curved electrode actuators *J. Microelectromech. Syst.* **6** 257–65
- [8] Li J, Brenner M P, Christen T, Kotilainen M S, Lang J H and Slocum A H 2005 Deep-reactive ion-etched compliant starting zone electrostatic zipping actuators *J. Microelectromech. Syst.* **14** 1283–97
- [9] Comtois J H and Bright V M 1997 Application for surface-micromachined polysilicon thermal actuators and arrays *Sensors Actuators A* **58** 19–25
- [10] Guckel H, Klein J, Christenson T, Skrobis K, Laudon M and Lovell E G 1992 Thermo-magnetic metal flexure actuators *Tech. Dig.: IEEE Solid-State Sensor and Actuator Workshop (New York, USA)* pp 73–5
- [11] Que L, Park J-S and Gianchandani Y B 2001 Bent-beam electrothermal actuators: Part I. Single beam and cascaded devices *J. Microelectromech. Syst.* **10** 247–54
- [12] Que L, Otradovec L, Oliver A D and Gianchandani Y B 2001 Pulse and dc operation lifetimes of bent-beam electrothermal actuators *Tech. Dig.: MEMS 4th IEEE Int. Conf. on Micro Electro Mechanical Systems (Piscataway, NJ, USA)* pp 570–3
- [13] Park J-S, Chu L L, Oliver A D and Gianchandani Y B 2001 Bent-beam electrothermal actuators: Part II. Linear and rotary microengines *J. Microelectromech. Syst.* **10** 255–62
- [14] Lin L and Lin S H 1998 Vertically driven microactuators by electrothermal buckling effects *Sensors Actuators A* **71** 35–9
- [15] Chen W C, Chu C C, Hsieh J and Fang W 2003 A reliable single-layer out-of-plane micromachined thermal actuator *Sensors Actuators A* **103** 48–58
- [16] Ahn C H, Kim Y J and Allen M G 1993 A planar variable reluctance magnetic micromotor with fully integrated stator and coils *J. Microelectromech. Syst.* **2** 165–73
- [17] Guckel H 1998 High-aspect-ratio micromachining via deep x-ray lithography *Proc. IEEE* **86** 1586–93
- [18] Ko J S, Lee M L, Lee D S, Choi C A and Kim Y T 2002 Development and application of a laterally driven electromagnetic microactuator *Appl. Phys. Lett.* **81** 547–9
- [19] Lagorce L K, Brand O and Allen M G 1999 Magnetic microactuators based on polymer magnet *J. Microelectromech. Syst.* **8** 2–9
- [20] Takagi K, Li J-F, Yokoyama S, Watanabe R, Almajid A and Taya M 2002 Design and fabrication of functionally graded PZT/Pt piezoelectric bimorph actuator *Sci. Technol. Adv. Mater.* **3** 217–24
- [21] Flynn A M, Tavrow L S, Bart S F, Brooks R A, Ehrlich D J, Udayakumar K R and Cross L E 1992 Piezoelectric micromotors *J. Microelectromech. Syst.* **1** 44–52
- [22] Gill J J and Carman G P 2000 Thin film NiTi shape memory alloy microactuator with two-way effect *Micro-Electro-Mechanical Systems (MEMS): ASME Int. Mechanical Engineering Congress and Exposition, (New York, USA)* pp 89–95
- [23] Tsai J-H and Lin L 2002 A thermal-bubble-actuated micronozzle-diffuser pump *IEEE/ASME J. Microelectromech. Syst.* **11** 665–71
- [24] Su Y-C, Lin L and Pisano A P 2002 A water-powered osmotic microactuator *IEEE/ASME J. Microelectromech. Syst.* **11** 736–42
- [25] Selvaganapathy P, Carlen E T and Mastrangelo C H 2002 Batch fabricated inline microfluidic valve *Solid-State Sensor, Actuator, and Microsystem Workshop (2–6 June)* pp 317–20
- [26] Cho H J and Ahn C H 2002 A bidirectional magnetic microactuator using electroplated permanent magnet arrays *J. Microelectromech. Syst.* **11** 78–84
- [27] Tabat N, Klein N and Guckel H 1997 Single flux-path bi-directional linear actuators *Int. Conf. on Solid-State Sensors and Actuators*
- [28] Yan D, Khajepour A and Mansour R 2004 Design and modeling of a MEMS bidirectional vertical thermal actuator *J. Micromech. Microeng.* **14** 841–50
- [29] Chiao M and Lin L 2000 Self-buckling of micromachined beams under resistive heating *J. Microelectromech. Syst.* **9** 146–51
- [30] MUMPS http://www.memscap.com/en_mumps.html
- [31] Kruglick E J J 1999 Microrelay design, performance, and systems *PhD Dissertation* University of California at Berkeley
- [32] Cao A, Yuen P and Lin L 2007 Micro-relays with bi-directional electrothermal electromagnetic actuators and liquid metal wetted contacts *J. Microelectromech. Syst.* at press